

A *BCL-2*-related gene is activated in avian cells transformed by the Rous sarcoma virus

G.Gillet¹, M.Guerin², A.Trembleau³ and G.Brun

Laboratoire de Biologie Moléculaire et Cellulaire, UMR 49 CNRS, LA-INRA, ENS Lyon, 46 allée d'Italie, F-69364 Lyon Cédex 07, France

²Present address: CBM, Université d'Orléans, 1 avenue de la recherche scientifique, F-45071 Orléans Cédex, France

³Present address: URA 1414 CNRS, ENS, 46 rue d'Ulm, F-75230 Paris Cédex 05, France

¹Corresponding author

Communicated by F.Cuzin

The oncoprotein p60^{v-src} encoded by the Rous sarcoma virus (RSV) genome is the prototype of non-receptor tyrosine kinases. More than 50 targets of p60^{v-src} have been described to date. However, the precise mechanisms of RSV transformation remain to be elucidated. Here, we present the study of a new v-src-activated gene, *NR-13*, which encodes a protein identified as a new member of the Bcl-2 family. This protein is localized in the membrane with a pattern already observed with Bcl-2. In quail embryos, this gene is mainly expressed in neural and muscular tissues. Its expression is dramatically down-regulated after embryonic day 7 (E7) in the optic tectum. To evaluate a possible role for *NR-13* in the control of apoptotic processes in this particular brain area, *in situ* hybridization and DNA ladder fractionation studies were performed to correlate *NR-13* expression with typical situations of apoptosis during brain development. Our results support the idea that RSV could activate anti-apoptotic functions of the host cell resulting in an increase of their lifespan, which could be particularly relevant to tumour formation.

Key words: BCL-2/Rous sarcoma virus/transformation

Introduction

The oncogene harboured by the Rous sarcoma virus (RSV) encodes a membrane-associated tyrosine kinase, p60^{v-src}, which accounts for the transforming properties of the virus (Jove and Hanafusa, 1987; Resh, 1994). Indeed, RSV mutants encoding an inactive tyrosine kinase or harbouring a copy of the proto-oncogene *c-src* instead of *v-src* are unable to transform cells (reviewed by Jove and Hanafusa, 1987; Brickell, 1992). The structures of p60^{v-src} and p60^{c-src} are now well understood and their major functional domains have been characterized. The two enzymes differ in the C-terminal region, which contains the major regulatory site for tyrosine kinase activity (Kaech *et al.*, 1993), and in a limited number of amino acid changes scattered along the protein sequence (reviewed by Jove and Hanafusa, 1987; Brickell, 1992).

p60^{c-src} is the prototype of a family of eight non-receptor tyrosine kinases which contain in the N-terminal region two domains of homology called SH2 and SH3 (SH for 'src homology') and an active site in the C-terminal halves (Brickell, 1992). The presence of these two domains in the same molecule allows p60^{c-src} to participate in a complex network of protein-protein interactions which is of particular relevance in signal transduction and in the determination of cell shape and adhesiveness properties (Mayer and Baltimore, 1993). The SH2 domain also participates in the regulation of p60^{c-src} tyrosine kinase activity. The last tyrosine residue located close to the C-terminal end (position 527 in the chick protein) can, when it is phosphorylated, bind to SH2 causing a folding of the molecule. In this conformation, access of ATP to the catalytic site is hindered and p60^{c-src} is inactive (reviewed by Cooper and Howell, 1993). Recent evidence suggests that the phosphorylation state of tyrosine 527, which is the major regulatory element of p60^{c-src} tyrosine kinase activity (Kaech *et al.*, 1993) could be controlled by a balance between the activities of the tyrosine kinase CSK (Sabe *et al.*, 1992) and of the phosphatase PTP α (Zheng *et al.*, 1992). During the M phase of the cell cycle, tyrosine 527 is dephosphorylated which consequently activates p60^{c-src} (reviewed by Taylor and Shalloway, 1993). PTP α also activates p60^{c-src} in differentiating neurones (den Hertog *et al.*, 1993). The oncoprotein p60^{v-src}, which is devoid of tyrosine 527, is constitutively active (reviewed by Brickell, 1992). Mutations at position 527 or in the SH2 domain of p60^{c-src} deregulate its activity, resulting in proteins which exhibit transforming properties (Hirai and Varmus, 1990; O'Brien *et al.*, 1990). Despite these recent data and the very abundant literature concerning *v-src*, the exact mechanism of cellular transformation by this oncogene still awaits complete elucidation (reviewed by Brickell, 1992).

The understanding of p60^{v-src} transformation mechanisms relies on the identification of its cellular targets. To date more than 50 proteins phosphorylated on tyrosine by p60^{v-src} have been described. They take part in intermediate metabolism, cell adhesion, cytoskeleton architecture, regulation of transcription and transduction of mitogenic or differentiation signals (reviewed by Brickell, 1992). Among all these proteins, it is still difficult to determine precisely the major intermediates in *v-src* action, but some of them seem to be particularly relevant to the cellular response to RSV infection. Indeed, the phosphorylation of two integrin subunits by p60^{v-src} could explain alterations in adhesiveness of RSV-transformed cells (Tapley *et al.*, 1989; Horvath *et al.*, 1990; Guan and Shalloway, 1992). If we refer to the cell cycle, it has recently been shown that p60^{v-src} is able to phosphorylate and to activate a histone H1 kinase different from p34^{cdc2} which is probably a new member of the cdk family (Sternberg

et al., 1993). Interestingly, $p34^{dc2}$ itself is not activated by $p60^{v-src}$ (Krek and Nigg, 1991).

The complementary strategy is the characterization of cellular genes whose expression is modified upon RSV transformation. Indeed, AP-1 DNA binding activity has been shown to increase in *v-src*-transformed cells (Welham *et al.*, 1990; Catling *et al.*, 1994) and the activation of transcription factors of the AP-1 family may, at least in part, account for the modifications of gene expression observed upon RSV infection. A large number of *v-src*-regulated genes have already been described (Bédard *et al.*, 1987; Michel *et al.*, 1989; Guermah *et al.*, 1990; Sugano *et al.*, 1987; Gillet *et al.*, 1993; see Brickell, 1992, for a review) and this approach is still promising (Jamal *et al.*, 1994; Li and Drucker, 1994; Yoon and Boettiger, 1994). However, many of these genes are probably activated or inhibited as a mere consequence of cellular transformation and it remains unclear which ones really perform a pivotal role in the appearance of the transformed phenotype.

We describe here a new *v-src*-activated gene, *NR-13*, that was first isolated from a cDNA library of RSV-infected quail neuroretina cells (Gillet *et al.*, 1993). It encodes a short protein of 177 amino acids sharing a significant homology with the oncoprotein Bcl-2. Importantly, this homology is particularly high in two regions corresponding to the two domains BH1 and BH2 (BH for 'Bcl-2 homology') that have been recently described as necessary, and possibly sufficient, for Bcl-2 to protect cells from programmed cell death (Yin *et al.*, 1994). We also present data on its developmental expression pattern in connection with situations of apoptosis during brain development. These data support the idea that the activation of the anti-apoptotic gene *NR-13* contributes to the increased lifespan of RSV-transformed cells.

Results

NR-13 induction by *v-src* in vitro and in vivo

We have previously reported the isolation of a set of genes activated in quail neuroretina cells as a consequence of RSV infection (Gillet *et al.*, 1993). We present here the study of one of these genes (formerly named *T13* in Gillet *et al.*, 1993), that we propose to call *NR-13* (NR for 'neuroretina'). As shown by Northern blotting experiments, this gene was activated in quail embryo neuroretina cells (QNR cells) and fibroblasts (QEF) transformed by a wild type strain of RSV in culture (Figure 1). Its expression was strictly correlated with the transforming ability of the virus since cells infected with the thermosensitive strain tsNY68 did not significantly express the gene at the non-permissive temperature (Figure 1, lane 3). This was further confirmed using the non-transforming RSV mutant NY315 which was unable to up-regulate *NR-13* expression (Figure 1, lane 6) in QEF. This mutant encodes a non-myristylated form of $p60^{v-src}$ with the same kinase activity as wild type $p60^{v-src}$ but which is not located in the vicinity of the plasma membrane. The phosphorylation of membrane-associated targets of $p60^{v-src}$ is therefore probably a prerequisite for the activation of this new gene. In addition, *NR-13* was also activated by $p60^{v-src}$ *in vivo* since the corresponding 1.7 kb transcript accumulated in tumours caused by RSV infection in chickens (Figure 2).

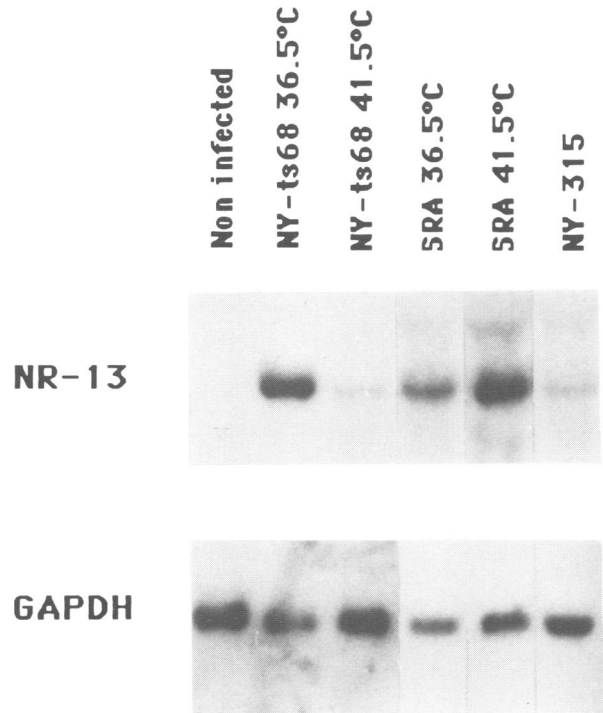


Fig. 1. RSV-induced expression of *NR-13* in QEF. Northern blots (10 μ g total RNA/lane) were probed with gel-purified *NR-13* cDNA radiolabelled by random priming. GAPDH was used for calibration. The size of *NR-13* transcript is 1.7 kb (Gillet *et al.*, 1993). The permissive and the non-permissive temperatures for the temperature sensitive mutant tsNY68 are 36.5°C and 41.5°C, respectively. When no temperature is indicated cells were grown at 36.5°C. SRA: wild type strain; tsNY68: temperature sensitive mutant; NY315: non-transforming mutant harbouring a non-myristylated form of $p60^{v-src}$.

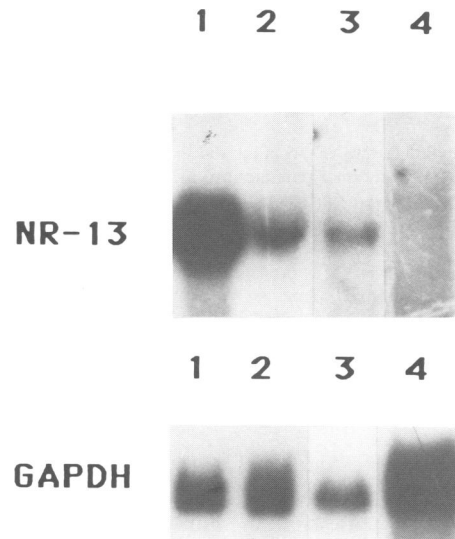


Fig. 2. Expression of *NR-13* in RSV-induced tumours in chickens. Northern blots (10 μ g per lane) were probed with 32 P-labelled *NR-13* cDNA and calibrated with GAPDH as in Figure 1. Lane 1, QEF infected by SRA grown at 36.5°C; lane 2, non-infected QEF; lane 3, chicken wing tumour caused by injection of a wild type viral suspension; lane 4, contralateral wing (non-injected) of the same animal. This experiment was reproduced with three different animals. The film has been overexposed to ensure that *NR-13* was absent from the normal tissue.

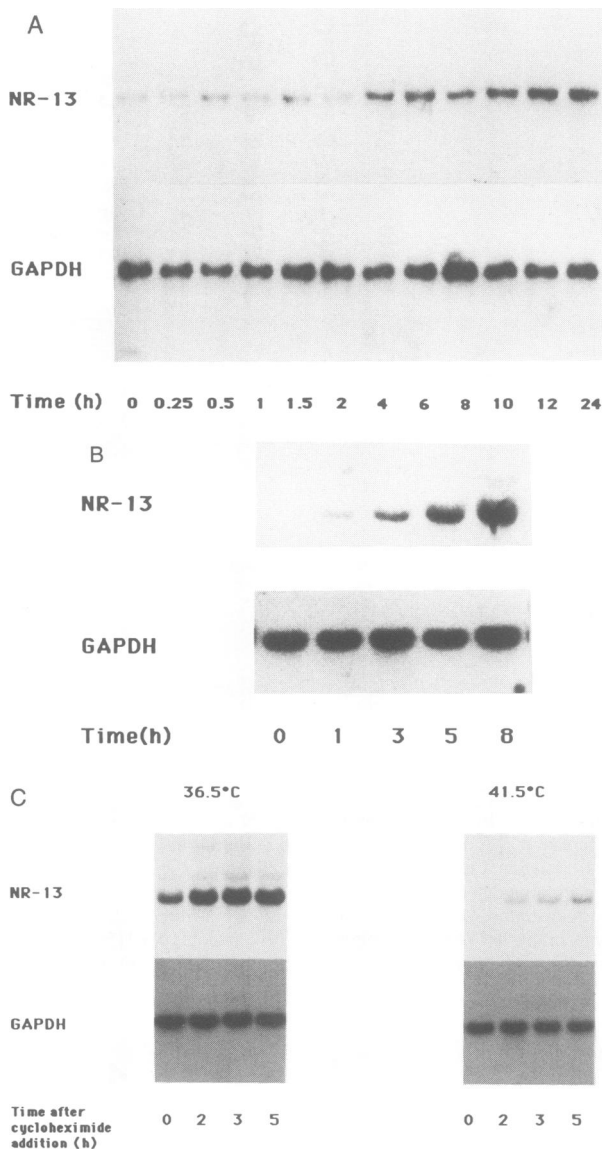


Fig. 3. Time course of *NR-13* induction in tsNY68-infected QEF following p60^{V-src} thermal renaturation. Effect of cycloheximide. Northern blotting were carried out with 10 µg of total RNA from tsNY68-infected QEF in each lane. The probes used were the same as in Figures 1 and 2. (A) QEF were grown for 48 h at 41.5°C and then placed at 36.5°C. RNA was prepared at the indicated times after the temperature change. (B) Same as (A), except that cycloheximide (10 µg/ml) was added 30 min before the temperature change to 36.5°C. (C) Effect of cycloheximide alone at 36.5°C and 41.5°C; total RNA was prepared at the indicated times following cycloheximide addition.

In tsNY68-infected quail embryo fibroblasts, *NR-13* expression was induced ~2 h after p60^{V-src} renaturation following a decrease from the non-permissive temperature to the permissive temperature (Figure 3A). *NR-13* transcript accumulation was also observed when this experiment was carried out in the presence of cycloheximide (Figure 3B), suggesting that p60^{V-src} was able to activate *NR-13* in the absence of protein synthesis. The possibility remains, however, that the accumulation observed in Figure 3B is merely an effect of cycloheximide itself and totally independent of *v-src*. Therefore, as shown in Figure 3C, we checked the influence of cycloheximide and found

```

          M P G S L K E E T 9
tgctcgggcccgcagccgcccgggcccgcggcc ATG CGG GGC TCT CTG AAG GAG GAG ACG 61
A L L L E D Y F Q H R A G G A A L P 27
GGC CTG CTG CTG GAG GAT TAC TTC CAG CAC CGG GCC GGC GGG GCC GCG CTG CCT 115
P S A T A A E L R R A A A E L E R R 45
CCG AGC GCC ACG GCG GCC GAG CTG GCG GCG GCG GCG GAG CTG GAG CGA CGG 169
E R P F F R S C A P L A R A E P R E 63
GAG CGG CCC TTC TTC CGA TCC TGC GCT CCG CTG GCG GCG GCG GAG CTG GAG 223
A A A L L R K V A A Q L E T D G G L 81
GCG GCG GCG CTG CTG GCG AAG GTG GCG GCG CAG CTG GAG ACC GAC GGC GGC CTG 277
N W G R L L A L V V F A G T L A A A 99
AAC TGG GGC CGG CTG CTG GCG CTC GTG GTG TTC GCC GGC ACG TTG GCG GCA GCG 331
L A E S A C E E G P S R L A A A L T 117
CTG GCC GAG AGC GCC TGC GAG GAA GGG CGG AGC CGC CTG GCC GCG GCG CTG A 385
A Y L A E E Q G E W M E E H G G W D 135
GCG TAC CTG GCC GAG GAG CAG GGA GAG TGG ATG GAG GAG CAC GGC GGA TGG GAT 439
G F C R F F G R H G S Q P A D Q N S 153
GGC TTC TGT GGC TTC GGC AGA CAT GGC TOC CAA CCA GCT GAC CAG AAC AGT 493
T L S N A I M A A A G F G I A G L A 171
ACC TTA AGC AAT GCT ATC ATG GCA GCA GCA GGG TTT GGA ATA GCA GGA TTA GCT 547
F L L V V R *
TTT CTC TTG GTG GTG GCG TAG gctgatggatggatggatgcttgcgaatgggaaagtactc 178
tgagaactgtttaccagattgcatctctattctatagaaacagatcctcaagaagaagtttatatttta 611
aagtggctggaaaacttgctcaccaaacccttggtctataaacgcgcttcaactcgtaccggtaacggcaca 755
aacgtgtaccaaaaccaccactttgtggtgttcacactgtgtcgtctccaaatgcccctggactttctt 827
ttgaactgttgaccctaaactgtaaccatggttctgtactgtaactctgatgctcaatgtcacgctagga 899
aaaagctatggtggactcgttaactaaaccctgtgttcaaggcatttcatgaggagcagctccagacactcgcc 971
tgccattcactgctaacgtggcctcacaccgactgatagaacacggtctgtggctcaccatgctgcccag 1043
caactgttatgagaggcaactcaactcgttggttgatgtagagcagtagtacctgtgatgtagggcgtta 1115
tggcttgatgtaagtgaaggctgatttcgatgacactacaagagtgtaagtggtgatacaggacagtaaggc 1187
tgcaattccagttcttactgaaaggatttgaataataaaccttaattggtatagtgaaatccagtgagggc 1259
tggaaattctctgatttcccttacaacacgagaattccatataatataatattttgagattttatc 1331
actgtataaactgtagccatgacatctttattttgtttaaactcatttttaagtgtgttcttctca 1403
ctctcatgtgtgcaggcgttgtctgttttgagaaattgtttgtctatttcaactgctgtgtattcttt 1475

```

Fig. 4. cDNA and protein sequence of *NR-13*. The coding sequence and the deduced amino acid sequence (one letter code) are in uppercase letters. The Kozak consensus sequence is in bold characters. The destabilizing ATTTA motifs are underlined.

that it could only slightly induce *NR-13* expression in cells maintained at a constant temperature. Taken together, these results clearly show that *NR-13* is induced by a mechanism independent of protein neosynthesis following p60^{V-src} renaturation. *NR-13* behaves therefore as a primary response gene and, as such, could perform an important role in the cellular response induced by this oncogene.

NR-13 is associated with the plasma membrane

Isolation of a 1.5 kb cDNA, ~200 bp shorter than the estimated mRNA length, suggested that most of the coding sequence was present in this clone. Indeed, the sequence depicted in Figure 4 (1475 nucleotides) appears entirely located upstream of the polyadenylation signal, lacking a short part of the 3' end and the poly(A) tail. This sequence exhibits a unique open reading frame of 531 nucleotides, starting at an AUG initiation codon surrounded by a degenerated Kozak consensus sequence (Lütcke *et al.*, 1987) and encoding a short protein of 177 amino acids (Figure 4). A prominent feature of this sequence is the very long 3' non-translated sequence with three putative destabilizing boxes and a short leader sequence. In addition to the presence of two conserved homology boxes which unambiguously identify this gene as a member of the *bcl-2* family (discussed later), a short hydrophobic region (residues 159–177) could correspond to a membrane-interacting domain. The predicted isoelectric point is 5.4 and this value has been confirmed by *in vitro* translation followed by isoelectrofocusing. Antibodies have been

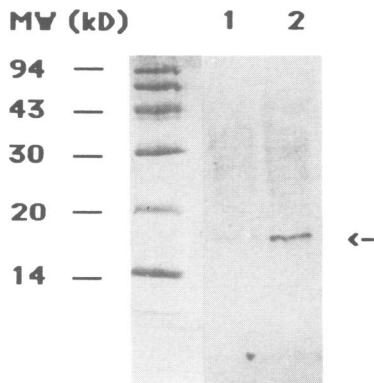


Fig. 5. Characterization of the NR-13 protein in QNR cells. Whole protein extract (10 μ g) from uninfected QNR cells (1) or QNR cells infected by RSV (2) were separated by SDS-PAGE and transferred onto a nitrocellulose membrane. The Western blot was probed with protein A-purified antibodies raised against a GST-NR-13 fusion protein. An 18 kDa protein (arrow) was revealed by autoradiography using the ECL detection system (Amersham). Position of mol. wt standards is indicated on the left.

raised against a GST-NR-13 fusion protein and were shown to cross-react with the *in vitro* translation product as expected (not shown). Western blotting using these antibodies showed that, in agreement with conclusions drawn from sequence data, a protein with an apparent molecular weight of 18–19 kDa is accumulated in *v-src*-transformed QNR cells compared with non-transformed cells (Figure 5).

An immunohistochemical approach helped to determine the subcellular localization of this protein. Figure 6B shows that, in RSV-transformed QEF, a fluorescent signal was detected in patches at the periphery of the cells but was absent from nuclei, suggesting that the NR-13 product is associated with the plasma membrane. As expected, no signal could be detected in non-transformed cells (Figure 6A, left panel). This observation agrees well with presence of the C-terminal hydrophobic region that could mediate interactions with the lipid bilayer (Figure 4). Alternatively, the NR-13 product could associate with a protein which is itself anchored to the plasma membrane.

NR-13 is a new member of the *Bcl-2* family

A remarkable feature of this predicted sequence is its significant homology with *Bcl-2* and all the *Bcl-2*-like proteins described to date (Vaux, 1993) as shown in Figure 7A. Computer-assisted alignment of amino acid sequences have shown that NR-13 and chicken *Bcl-2* (Eguchi *et al.*, 1992) share 25% identical amino acids and 47% conserved amino acids; for NR-13 and Bax (Oltvai *et al.*, 1993) these two values reach 28% and 54%, respectively. Remarkably, the extent of homology between all the *Bcl-2* family members is almost constant, suggesting that all these proteins have evolved at the same rate from a common ancestor (Figure 7B).

The relationship between NR-13 and the *Bcl-2* family is further substantiated by the high degree of conservation of the two boxes BH1 and BH2 (Yin *et al.*, 1994). These two regions are a typical feature of all the members of this family. Mutation studies have shown that they are involved in the formation of heterodimers between Bax and *Bcl-2* and that they are essential in regulating the

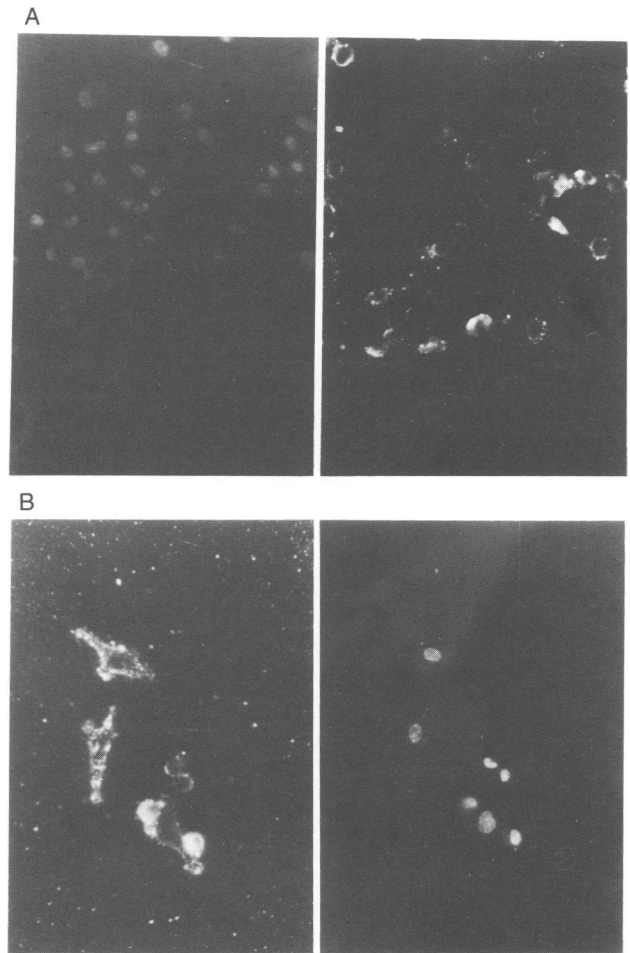


Fig. 6. Subcellular localization of NR-13 in QEF. Cells were fixed on glass slides and incubated with immunopurified anti-NR-13 antibodies. The NR-13 product was detected using an anti-rabbit secondary antibody coupled to fluoresceine (FITC). Slides were also incubated with Hoechst's reagent to label nuclei. (A) Left panel: uninfected QEF; right panel: RSV-infected QEF. (B) RSV-infected QEF at a higher magnification, left panel: the excited chromophore was FITC, right panel: same field irradiated at a shorter wavelength to visualize nuclei (Hoechst's chromophore).

anti-apoptotic function of *Bcl-2* (Oltvai *et al.*, 1993; Yin *et al.*, 1994). These data clearly identify NR-13 as a new *Bcl-2*-like protein. They also suggest that NR-13 may be involved in the regulation of apoptosis in avian cells.

Expression of NR-13 during development of the quail embryo

As a first step towards the determination of the function of *NR-13*, we analysed its expression during the development of quail embryos between E5 and E17 (hatching). The Northern blots depicted in Figure 8 show that *NR-13* expression was very low in liver, cerebellum and striatum, more abundant in heart, striated muscle and retina, and highest in the optic tectum at E6 and E7. In this particular brain area, *NR-13* expression was clearly developmentally regulated since it was almost completely switched off between E7 and E8 and remained very low afterwards. During this period, most cells of the tectum perform their last mitosis (LaVail and Cowan, 1971b; Senut and Alvarado-Mallart, 1986). *In situ* hybridization experiments were carried out to determine whether NR-13 down-

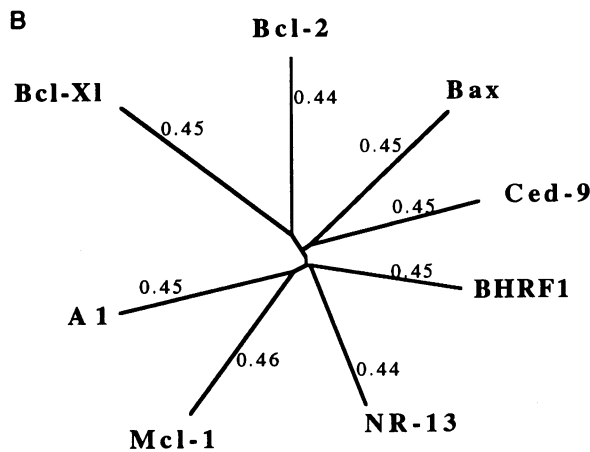
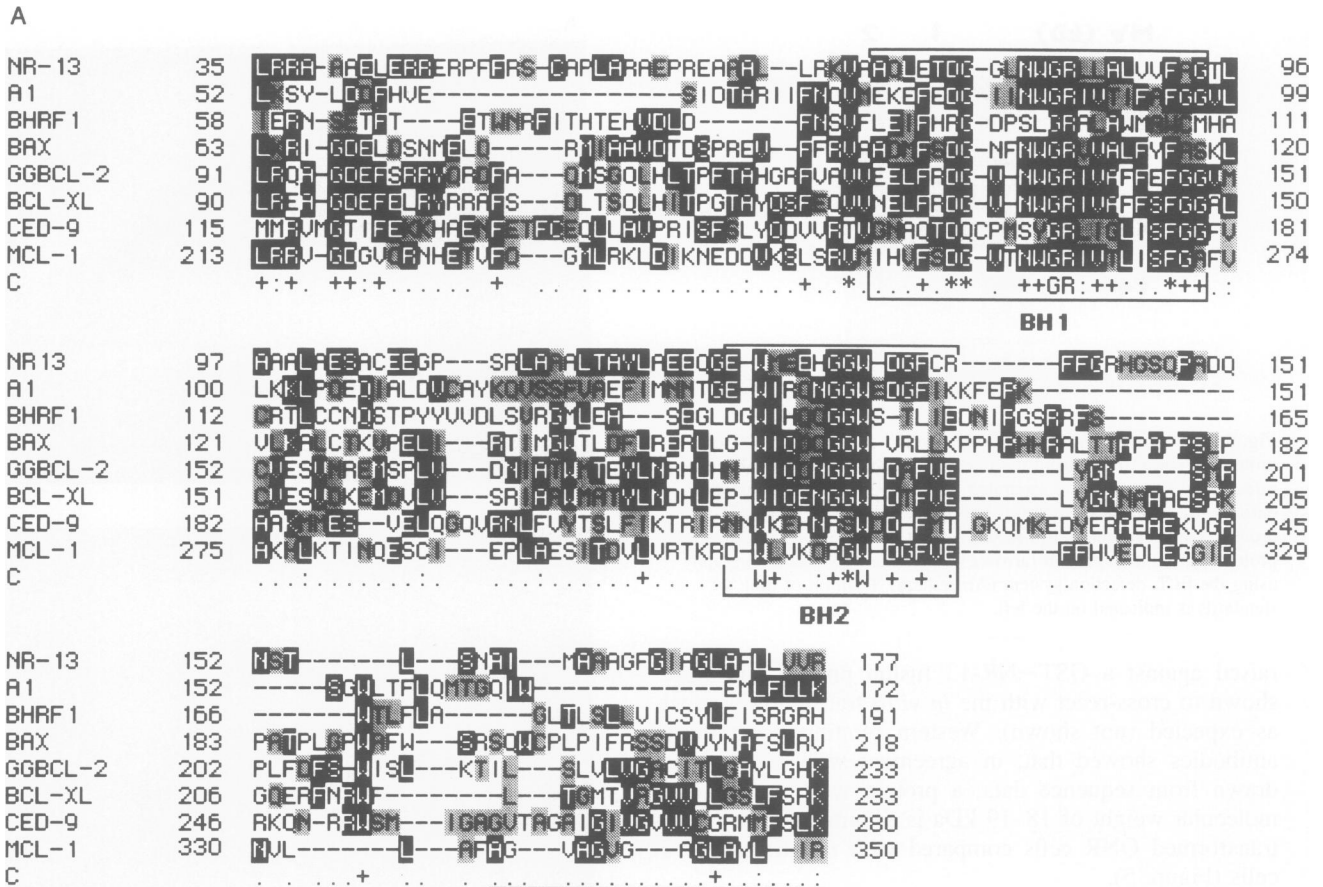


Fig. 7. (A) Amino acid alignment of the C-terminal regions of the various Bcl-2 family members. NR-13, A1 (Lin *et al.*, 1993), BHRF1 (Pearson *et al.*, 1987), Bax (Oltvai *et al.*, 1993), chicken Bcl-2 (Eguchi *et al.*, 1992), Bcl-xl (Boise *et al.*, 1993), Ced-9 (Hengartner and Horvitz, 1994), MCL-1 (Kozopas *et al.*, 1993). Numbers indicate amino acid positions. Identical residues are in black; conserved residues are shaded. For this purpose, the following sets of amino acids are considered similar: G, A, C, S, T; E, D, Q, N; R, K, H; V, M, L, I; F, Y, W. Boxes demonstrate the two Bcl-2 homology domains; the C-terminal hydrophobic region of Bcl-2 is underlined. Consensus line (C): two or three identical residues of eight, '+'; four identical residues, '+'; five or six identities, '+'; seven identities, '*'; a letter indicates eight of eight identities. (B) Diagram showing the evolutionary distances between several members of the Bcl-2 family. This is an unrooted tree. Numbers are in arbitrary units. Example of calculation: the distance between NR-13 and BHRF1 is: 0.44 + 0.45 = 0.89, whereas between NR-13 and Bcl-2 it is: 0.44 + 0.44 = 0.88 and between BHRF1 and Bcl-2 it is: 0.45 + 0.44 = 0.89. The three values are very close, indicating that these three proteins are equally distant from one another.

regulation could be correlated with this arrest of cell proliferation. Figure 9 shows that, at E6–E7, NR-13 transcript was mainly localized in the neural epithelium, which is the innermost layer of the tectum. Previous investigations have shown that, at this stage, most dividing cells are localized in layer VI which is a more external region of the tectum (LaVail and Cowan, 1971a,b); our data indicated therefore that NR-13 expression does not correlate with the mitotic activity of the various layers of the tectum. Thus, it appears unlikely that the reduction of NR-13 expression observed between E7 and E8 is linked to the arrest of cell divisions in the developing optic tectum.

In view of the homology between NR-13 and Bcl-2,

we investigated whether NR-13 expression could be related to cell death events occurring during the development of the tectum. Hence, we analysed the kinetics of apoptosis in the developing tectum by the detection of nucleosome-sized DNA ladders that are typical of apoptotic cells (Rösl, 1992). Remarkably, as shown in Figure 10, such ladders appeared at E8—the day after NR-13 expression was switched off—peaked at E13–14 and started to disappear at hatching (E17). The ladders were no longer observed in adults (Figure 10). These observations strongly suggest that NR-13 down-regulation is an event required for the onset of apoptosis in the developing optic tectum.

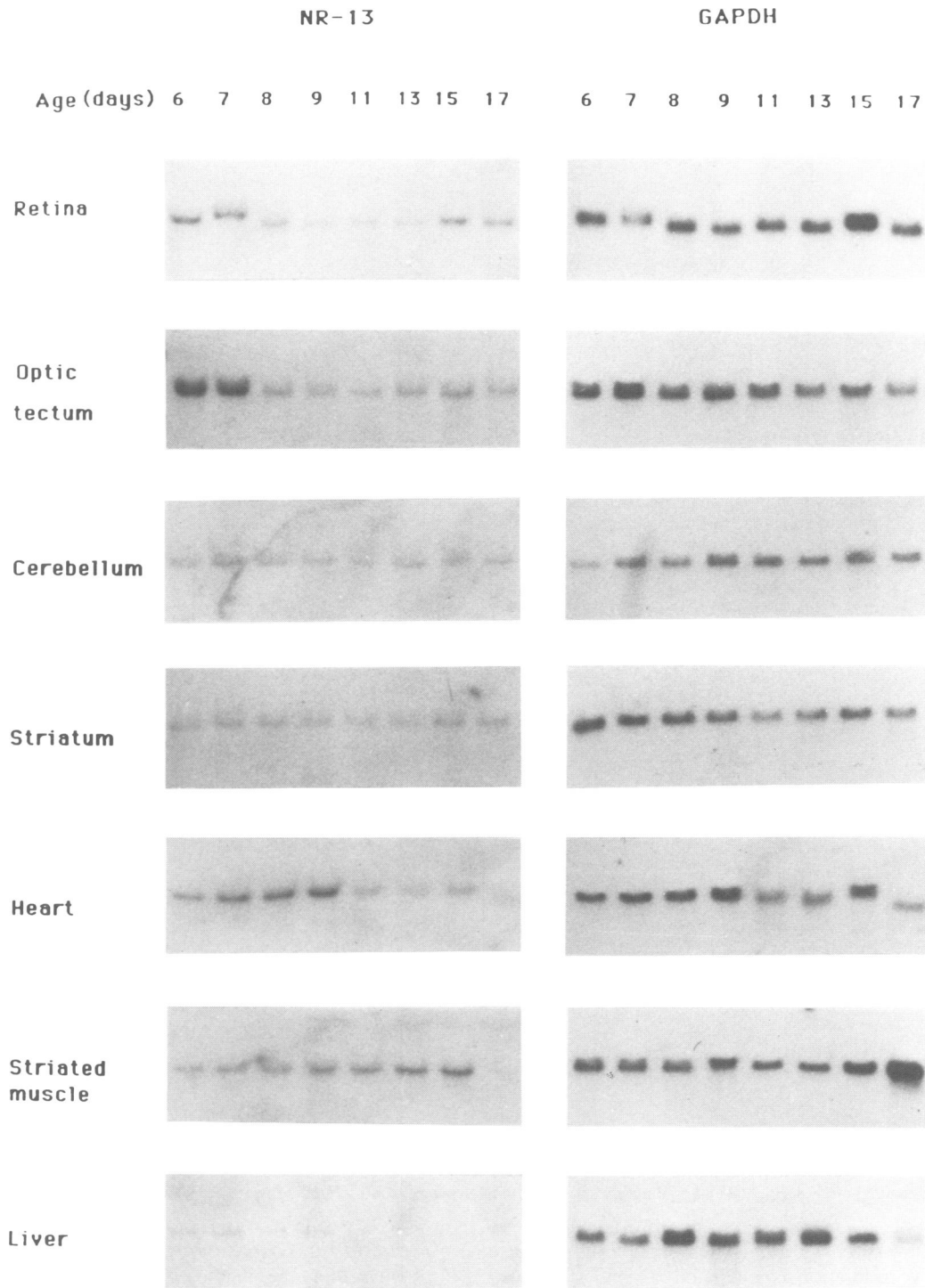


Fig. 8. Northern analysis of *NR-13* expression during development. RNA was prepared from embryonic day E5 to E17 (hatching). Northern blots (10 µg per lane) of total RNA from different organs were probed with *NR-13* cDNA and reprobbed with *GAPDH* for calibration. This is a typical result of at least three experiments.

Discussion

The role of non-receptor tyrosine kinases, in particular *v-src*, in the control of cellular anti-apoptotic functions has become a subject of interest since the finding that phosphatase 2A is inactivated in *v-src*-transformed fibroblasts (Chen *et al.*, 1994). Indeed, the phosphatase inhibitor okadaic acid is likely to block programmed cell

death mechanisms by inhibiting phosphatase 2A activity (Baxter and Lavin, 1992). These data strongly suggest that *v-src* itself could block apoptosis, since it has the same effect as okadaic acid on phosphatase 2A activity, and are also in agreement with recent data indicating that *v-src* has an anti-apoptotic effect on MDCK cells (Frish and Francis, 1994). Karin's group had already proposed that *c-src* could protect cells against UV-induced

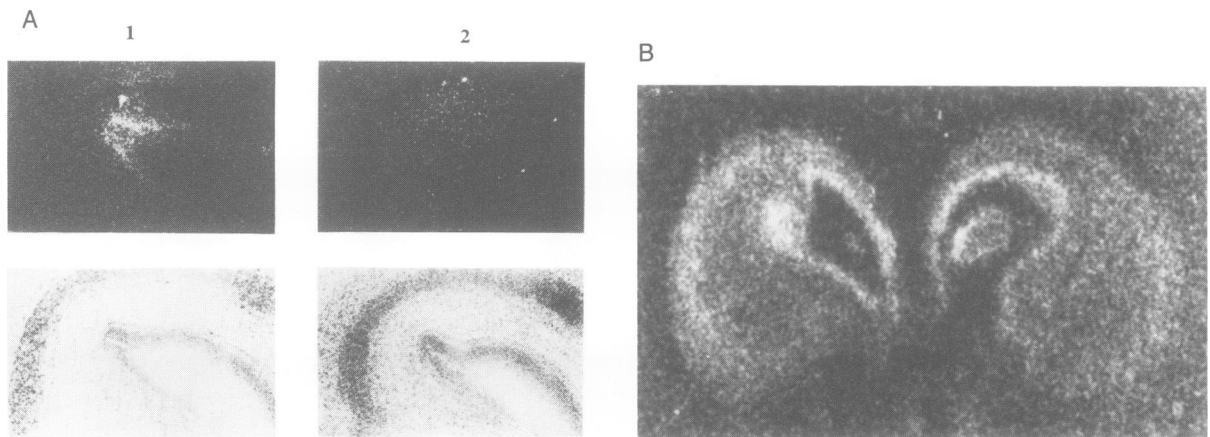


Fig. 9. *In situ* analysis of *NR-13* expression in the developing brain. Horizontal sections from E7 brains were hybridized with antisense or sense (negative control) ^{32}P -labelled *NR-13* riboprobes. Slides were autoradiographed for 1 week and the film was photographed by a computer-coupled camera. The slides were then dipped in a photographic emulsion and kept in the dark room for 4 weeks before development and microscopic analysis. (A) Darkfield photograph of the emulsion after 1 month exposure of the E7 sections; only one optic lobe is shown. (1) antisense probe; (2) sense probe (negative control). Top: dark field microphotographs; bottom: haematoxylin-eosin staining. (B) Computerized image of the autoradiogram obtained after 1 week's exposure of the tissue section hybridized with the antisense probe, showing the pattern of *NR-13* expression in the two optic lobes; silver grains appear in white.

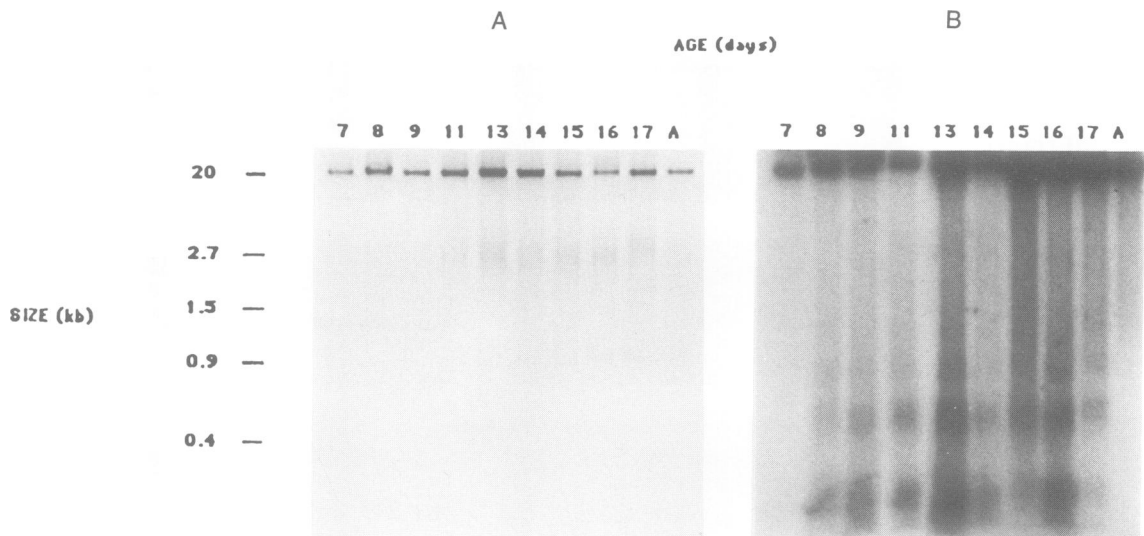


Fig. 10. Kinetics of genomic DNA fragmentation in the developing optic tectum. 3' ends of genomic DNA (1 $\mu\text{g}/\text{lane}$) from quail optic tectum dissected at the indicated embryonic days were radiolabelled with ^{32}P using the Klenow fragment of *Escherichia coli* DNA polymerase I according to Rösl (1992). DNA fragments were separated on a 2% agarose gel. The gel was dried and autoradiographed. (A) Photograph of the gel stained with ethidium bromide before drying. (B) autoradiogram showing the nucleosome-sized DNA fragments.

cell death (Devary *et al.*, 1992). This apoptotic response following UV irradiation is mediated by p53 (reviewed by Williams and Smith, 1993) and it has been recently reported that Bcl-2 is able to block p53-induced programmed cell death (Chiou *et al.*, 1994). Thus, we can also imagine that *c-src* could protect cells against UV-induced apoptosis by activating *bcl-2*, possibly through the inhibition of phosphatase 2A. According to this speculative model, *c-src* alone should be able to activate *bcl-2* or another anti-apoptotic gene.

In this paper we report the characterization of a new gene activated by *v-src*, the transforming counterpart of *c-src*. This gene codes for a protein which has significant homologies with the members of the rapidly growing Bcl-2 family (Vaux, 1993) and is therefore a good candidate to mediate a possible anti-apoptotic effect of *v-src*.

Induction of *NR-13* expression by *v-src*

$\text{p60}^{\text{v-src}}$ must be anchored into the plasma membrane to up-regulate *NR-13* since the non-myristylated mutant NY315 had no effect on *NR-13* transcript accumulation in fibroblasts (Figure 1). Since NY315 is a non-transforming mutant of RSV (Pellman *et al.*, 1985), this suggests that *NR-13* participates in the establishment of the transformed phenotype due to RSV infection of avian cells in culture. In addition, the fact that *NR-13* is also activated in RSV-induced tumours in chicken suggests that it performs a role in tumorigenesis *in vivo* (Figure 2). Interestingly, serum growth factors also appear able to induce *NR-13* expression to some extent since its transcript could be detected in QEF in culture but not in normal muscular tissue *in vivo* (Figure 2, compare lanes 2 and 4). Concerning the mechanism of *NR-13* induction by *v-src*,

previous run-on experiments indicated that *v-src* had little effect on *NR-13* transcription rate (Gillet *et al.*, 1993). Moreover, in tsNY68-infected QEF, we have shown that decay of *NR-13* transcripts is significantly slower at the permissive temperature than at the non-permissive temperature (results not shown), suggesting also that the induction of *NR-13* in *v-src*-transformed cells is mainly due to a stabilization of the transcript.

NR-13: a new member of the Bcl-2 family

The cDNA sequence indicates that the clone we have isolated exhibits a unique open reading frame encoding a putative protein of 177 amino acids (Figure 4). This has been confirmed by Western blotting using specific antibodies (Figure 5). The NR-13 protein has a C-terminal hydrophobic tail which suggests that it can bind to the plasma membrane (Figure 7). Immunohistochemistry experiments in QEF support this conclusion (Figure 6). The most important finding is that NR-13 shares a significant homology with all the Bcl-2-like proteins described to date (Vaux, 1993). The main feature of this family is the presence of two highly conserved regions, BH1 and BH2 (Figure 7A), which are essential for the inhibition of apoptosis by Bcl-2 (Yin *et al.*, 1994). However, the presence of BH1 and BH2 does not allow a role for NR-13 as an anti-apoptotic factor to be assumed. Indeed, these two domains are also found in both Bax and Bcl-2, two proteins which have opposite effects on cell death (Oltvai *et al.*, 1993). Moreover, the protein Bclx-s which is devoid of BH1 and BH2 domains behaves as an antagonist of Bcl-2 (Boise *et al.*, 1993). It appeared therefore essential to correlate *NR-13* expression with well identified physiological processes of cell death.

In the nervous system, where intense proliferation waves precede programmed cell death (reviewed by Oppenheim, 1991), the highest expression of *NR-13* is detected in the optic tectum at E6 and E7 (Figure 8). *In situ* hybridization data have shown that at this time *NR-13* is mainly expressed in the neural epithelium of the tectum whereas it is almost absent from the more external layers V and VI where most cell divisions are occurring (LaVail and Cowan, 1971a,b; see also Senut and Alvarado-Mallart, 1986). These data indicate that *NR-13* expression is not correlated with the mitotic activity of neural cells in the developing optic tectum.

In this particular brain area the proliferation phase ends at E7. From E8 to E14 various postmitotic precursors migrate to their definitive location and differentiate, leading to a considerable increase in the number of cellular layers (Senut and Alvarado-Mallart, 1986). In the nervous system, these periods of maturation are characterized by cell death events corresponding to the stabilization of functional connections (Oppenheim, 1991). We found DNA ladders typical of apoptotic cells (see e.g. Wood *et al.*, 1993) in the tectum between E8 and E17 with a peak at E13–14 (Figure 10). Remarkably, the appearance of DNA ladders follows the extinction of *NR-13* expression (compare Figure 8 with Figure 10). This suggests that this gene could perform in the optic tectum a role similar to that of *bcl-2* in lymphoid cells (Strasser *et al.*, 1991; Nunez *et al.*, 1991; Borzillo *et al.*, 1992; Merino *et al.*, 1994). In addition, in NYts68-infected QNR cells in culture, the down-regulation of *NR-13* that follows p60^{v-src}

inactivation at 41.5°C, is also correlated with the appearance of nucleosome-sized DNA ladders (our unpublished results). The anti-apoptotic role of *NR-13* needs to be further confirmed, in particular by testing the effect of *NR-13* overexpression in cellular models of programmed cell death in culture. The results reported in this paper, showing for the first time that *v-src* regulates a *bcl-2*-like gene, provide further experimental support for the idea that the tumorigenic effect of RSV is mediated by a stimulation of the anti-apoptotic functions of the host cell, leading to abnormal cell accumulation.

Materials and methods

Cells and viruses

Fibroblasts and neuroretina cells were prepared from 7-day-old quail embryos (*Coturnix coturnix japonica*) and infected with the temperature sensitive RSV strain tsNY68 as previously described (Gillet *et al.*, 1993). QNR cells were grown and passaged in Eagle's basal medium supplemented with 8% fetal calf serum. Fibroblasts were grown in CEF medium (1× Ham's F10, 3 g/l tryptose phosphate broth, 0.2% sodium bicarbonate, 5% fetal calf serum, 1% chicken serum) supplemented with penicillin–streptomycin. The wild type Schmidt–Ruppin A strain of RSV and the temperature sensitive mutant tsNY68 were used as previously described (Gillet *et al.*, 1993) and the non-transforming mutant NY315 (Pellman *et al.*, 1985) was a kind gift from Dr H. Hanafusa (Rockefeller University, New York).

NR-13 cDNA cloning and sequencing

NR-13 cDNA was isolated by screening a quail neuroretina cell cDNA library (Gillet *et al.*, 1993) and the entire open reading frame was reconstituted from clones isolated by repeated screenings of this library and of a quail genomic library. A full length chick cDNA clone was directly isolated from a *v-src*-transformed chick embryo fibroblasts cDNA library (a kind gift from Dr A. Bédard). This clone had the same open reading frame as the reconstructed full length quail cDNA clone. The entire sequence of the cDNA was determined as described previously (Michel *et al.*, 1989).

RNA purification and Northern blots

Cells and tissue samples were rapidly frozen in liquid nitrogen and subsequently homogenized in 2–4 ml of guanidium isothiocyanate buffer (5 M guanidium isothiocyanate, 10 mM EDTA, 50 mM Tris, pH 7.5; 8% β-mercaptoethanol). Each lysate was then mixed with 16 ml of a cold 4 M LiCl solution and kept overnight on ice. RNA was pelleted by centrifugation (30 min, 10 000 r.p.m. in a JS 13 Beckman rotor). The RNA pellet was resuspended in a phenol-saturated saline buffer (10 mM Tris, pH 7.5; 1 mM EDTA, pH 8; 0.1% SDS; 5% Tris-saturated phenol). After phenol–chloroform extraction, the RNA was precipitated with ethanol and resuspended in sterile H₂O. Northern blots were performed as previously described (Gillet *et al.*, 1993). ³²P-labelled probes were obtained from gel-purified cDNA inserts using the Amersham random priming kit.

Antibodies

Full length quail cDNA was cloned in the *EcoRI* site of pGEX2 (Pharmacia) to produce a GST–NR-13 fusion protein. The fusion protein was prepared as described in the pGEX vectors user's guide (Pharmacia). Rabbits were immunized by repeated intradermal injection of the fusion protein following standard techniques (Harlow and Lane, 1988). Serum was collected 15 days after the last injection and stored at –20°C.

In Western blotting experiments, the peroxidase-coupled secondary anti-rabbit antibody was purchased from Amersham (ECL detection system). Immunoglobulins of the rabbit serum were purified on a protein A–agarose affinity column using standard techniques (Harlow and Lane, 1988).

In immunohistochemistry experiments, the FITC-coupled anti-rabbit antibody was purchased from Sigma. Specific anti-NR-13 antibodies were further purified as follows: protein A-purified immunoglobulins were loaded onto an affinity column composed of glutathione transferase (GST) immobilized on glutathione beads (Pharmacia) and equilibrated with phosphate buffered saline (PBS). The material excluded from the column (pass through) was collected and loaded on to a second affinity

column in which the GST-NR-13 fusion protein was fixed to glutathione-coupled to agarose beads. This column was then washed with 10 vol PBS and the specific anti-NR-13 antibodies were eluted with 0.1 M triethylamine (pH 2.5). Fractions (100 μ l) were collected in Eppendorf tubes containing 10 μ l Tris 1 M (pH 8). The protein content of each fraction was determined with Bradford's reagent (Bio-Rad). Purified antibodies were pooled and stored at -20°C . The entire procedure was carried out at 4°C .

Western blots

SDS-PAGE was performed on a 17% polyacrylamide gel according to the standard technique of Laemmli (1970). After transfer onto nitrocellulose (BA 85, Schleicher and Schuell) and blocking with 5% low fat dried milk, the blot was incubated overnight at 4°C with the anti-NR-13 antibody. After incubation for 1 h with anti-rabbit peroxidase-coupled secondary antibody at room temperature chemiluminescence was detected according to the standard ECL protocol (Amersham).

In situ hybridization

Glass slides were pretreated with 1% 3-aminopropyltriethoxysilane (Fluka) in acetone. Cryosections (20 μm) from fresh-frozen quail embryo brains were thawed onto treated slides, fixed in 4% paraformaldehyde (30 min at room temperature) and rinsed three times (5 min each) in PBS. The sections were then acetylated and dehydrated in ethanol as previously described (Simmons *et al.*, 1989). Following hybridization, tissue sections were incubated overnight at 50°C in hybridization buffer (50% formamide, 10 mM Tris, pH 8, 0.3 M NaCl, 1 mM EDTA, $1\times$ Denhardt's, 0.5 mg/ml tRNA) containing the radioactive probe (10^6 c.p.m./ml). After hybridization, sections were washed four times (5 min each) in $2\times$ SSC and treated with RNase (30 min at 37°C) in a buffer containing 10 mM Tris, pH 8, 0.5 M NaCl, 1 mM EDTA and 0.02 mg/ml RNase A (Sigma). Sections were then washed at room temperature as follows: $2\times$ SSC, 5 min twice; $1\times$ SSC, 10 min; $0.5\times$ SSC, 10 min; followed by a final wash at 60°C in $0.2\times$ SSC. After a short rinse in $0.1\times$ SSC at room temperature, the samples were dehydrated in ethanol and air dried. Slides were autoradiographed for 1 week. Once the film (β -max, Amersham) had been developed, the slides were dipped into a photographic emulsion (Ilford) and revealed after 4 weeks' exposure. The two riboprobes (sense and antisense) were ^{32}P -labelled using the Boehringer *in vitro* transcription kit with SP6 or T7 primers using a DNA template which contained the first 500 nucleotides of the full length NR-13 cDNA cloned into the polylinker region of pBSK. The labelled riboprobes were purified by filtration on a Sephadex G50 column.

Immunohistochemistry

QEF were grown on glass slides, fixed in paraformaldehyde (2% in PBS) for 15 min and incubated for 10 min in a Triton X-100 solution (0.1% in PBS). After three washes in PBS (5 min each) the samples were incubated in PBS containing 20% normal goat serum for 1 h followed by incubation with the immunopurified anti-NR-13 antibody for 2 h. After three extensive washes with PBS (15 min each), the slides were incubated with the secondary antibody (anti-rabbit, coupled to FITC, Sigma) for 1 h; Hoechst's reagent (0.5 $\mu\text{g}/\text{ml}$, Sigma) was added at this step. The samples were then rinsed three times (15 min each) and fixed in 50% glycerol containing 2.5% DABCO (Sigma) to reduce fading. Samples were irradiated at 495 nm (FITC) or at 360 nm (Hoechst).

DNA ladders

Genomic DNA from quail optic tectum was prepared using standard techniques (Ausubel *et al.*, 1994). To visualize nucleosome-sized DNA ladders, 1 μg of each DNA sample was treated as described (Rösl, 1992).

Computer-assisted analysis of sequences

Protein sequences were compared using the Clustal V multialignment program. The unrooted phylogenetic tree shown in Figure 7B was obtained by the neighbour-joining method (Saitou and Nei, 1987).

Acknowledgements

We wish to thank Dr H.Hanafusa (Rockefeller University, New York, USA) for the RSV mutant NY-315 and Dr P.A.Bédard (York University, North York, Canada) for the chicken fibroblast cDNA library. We also want to thank Dr M.Lapadat Tapolski, Dr J.Samarut and Dr A.Sergeant (Ecole Normale Supérieure, Lyon) for their critical reading of the manuscript. We are indebted to Dr M.Gouy (Université Claude Bernard,

Lyon) and to Dr G.Deléage (Institut de Biologie et de Chimie des Protéines, Lyon) for their advice during the computer-assisted analysis of sequences. Stimulating discussions with Dr D.Michel (Ecole Normale Supérieure, Lyon) and Dr M.Volovitch (Ecole Normale Supérieure, Paris) were particularly helpful during the initial steps of this work. Our laboratory is supported by grants from Association pour la Recherche sur le Cancer and Fédération des Centres de Lutte contre le Cancer.

Accession number

The EMBL Data Library accession number is X84418.

References

- Ausubel, F.M. *et al.* (1994) In Janssen, K. (ed.), *Current Protocols in Molecular Biology*. Wiley & Sons, Boston, MA, pp. 221–222.
- Baxter, G.D. and Lavin, M.F. (1992) *J. Immunol.*, **148**, 1949–1954.
- Bédard, P.A., Alcorta, D., Simmons, D.L., Luk, K.C. and Erickson, L.R. (1987) *Proc. Natl Acad. Sci. USA*, **84**, 6715–6719.
- Boise, L.H. *et al.* (1993) *Cell*, **74**, 597–608.
- Borzillo, G.V., Endo, K. and Tsujimoto, Y. (1992) *Oncogene*, **7**, 869–876.
- Brickell, P.M. (1992) *Crit. Rev. Oncogenesis*, **3**, 401–446.
- Catling, A.D., Fincham, V.J., Framma, M.C., Haefner, B. and Wyke, J.A. (1994) *J. Virol.*, **68**, 4392–4399.
- Chen, J., Parsons, S. and Brautigan, D.L. (1994) *J. Biol. Chem.*, **269**, 7957–7962.
- Chiou, S.K., Rao, L. and White, E. (1994) *Mol. Cell. Biol.*, **14**, 2556–2563.
- Cooper, J.A. and Howell, B. (1993) *Cell*, **73**, 1051–1054.
- den Hertog, J., Pals, C.E.G.M., Peppelenbosch, M.P., Tertoolen, L.G.L., de Laat, S.W. and Kruijer, W. (1993) *EMBO J.*, **12**, 3789–3798.
- Devary, Y., Gottlieb, R.A., Smeal, T. and Karin, M. (1992) *Cell*, **71**, 1081–1091.
- Eguchi, Y., Ewert, D. and Tsujimoto, Y. (1992) *Nucleic Acids Res.*, **20**, 4187–4192.
- Frish, S.M. and Francis, H. (1994) *J. Cell Biol.*, **124**, 619–626.
- Gillet, G. *et al.* (1993) *Oncogene*, **8**, 565–574.
- Guan, J.L. and Shalloway, D. (1992) *Nature*, **358**, 690–692.
- Guermah, M., Gillet, G., Michel, D., Laugier, D., Brun, G. and Calothy, G. (1990) *Mol. Cell. Biol.*, **10**, 3584–3590.
- Harlow, E. and Lane, D. (1988) *Antibodies: A Laboratory Manual*. Cold Spring Harbor Laboratory Press, Cold Spring Harbor, NY, pp. 108 and 309.
- Hengartner, M.O. and Horvitz, H.R. (1994) *Cell*, **76**, 665–676.
- Hirai, H. and Varmus, H.E. (1990) *Mol. Cell. Biol.*, **10**, 1307–1318.
- Horvath, A.R., Elmore, M.A. and Kellie, S. (1990) *Oncogene*, **5**, 1349–1357.
- Jamal, H.H., Cano-Gauci, D.F., Buick, R.N. and Filmus, J. (1994) *Oncogene*, **9**, 417–423.
- Jove, R. and Hanafusa, H. (1987) *Annu. Rev. Cell Biol.*, **3**, 31–56.
- Kaech, S., Schnierle, B., Wyss, A. and Ballmer-Hofer, K. (1993) *Oncogene*, **8**, 575–581.
- Kozopas, K.M., Yang, T., Buchan, H.L., Zhou, P. and Craig, R.W. (1993) *Proc. Natl Acad. Sci. USA*, **90**, 3516–3520.
- Krek, W. and Nigg, E.A. (1991) *EMBO J.*, **10**, 305–316.
- Laemmli, U.K. (1970) *Nature*, **227**, 680–685.
- LaVail, J. and Cowan, M.W. (1971a) *Brain Res.*, **28**, 391–419.
- LaVail, J. and Cowan, M.W. (1971b) *Brain Res.*, **28**, 421–441.
- Li, X. and Drucker, D.J. (1994) *J. Biol. Chem.*, **269**, 6263–6266.
- Lin, E.Y., Orlofsky, A., Berger, M.S. and Prystowsky, M.B. (1993) *J. Immunol.*, **151**, 1979–1988.
- Lütcke, H.A., Chow, K.C., Mickel, F.S., Moss, K.A., Kern, H.F. and Scheele, G.A. (1987) *EMBO J.*, **6**, 43–48.
- Mayer, B.J. and Baltimore, D. (1993) *Trends Cell Biol.*, **3**, 8–13.
- Merino, R., Ding, D., Veis, D.J., Korsmeyer, S.J. and Nunez, G. (1994) *EMBO J.*, **13**, 683–691.
- Michel, D., Gillet, G., Volovitch, M., Pessac, B., Calothy, G. and Brun, G. (1989) *Oncogene Res.*, **4**, 127–136.
- Nunez, G., Hockenbery, D., McDonnell, T.J., Sorensen, C.M. and Korsmeyer, S.J. (1991) *Nature*, **353**, 71–73.
- O'Brien, M.C., Fukui, Y. and Hanafusa, H. (1990) *Mol. Cell. Biol.*, **10**, 2855–2862.
- Oltvai, Z., Millman, C.L. and Korsmeyer, S.J. (1993) *Cell*, **74**, 609–619.
- Oppenheim, R.W. (1991) *Annu. Rev. Neurosci.*, **14**, 453–501.
- Pearson, G.R., Luka, J., Petti, L., Sample, J., Birkenbach, M., Braun, D. and Kieff, E. (1987) *Virology*, **160**, 151–161.
- Pellman, D., Garber, F.R. and Hanafusa, H. (1985) *Proc. Natl Acad. Sci. USA*, **82**, 1623–1627.

- Resh, M.D. (1994) *Cell*, **76**, 411–413.
- Rösl, F. (1992) *Nucleic Acids Res.*, **20**, 5243.
- Sabe, H., Knudsen, B., Okada, M., Nada, S., Nakagawa, H. and Hanafusa, H. (1992) *Proc. Natl Acad. Sci. USA*, **89**, 2190–2194.
- Saitou, N. and Nei, M. (1987) *Mol. Biol. Evol.*, **4**, 406–425.
- Senut, M.C. and Alvarado-Mallart, R.M. (1986) *Dev. Brain Res.*, **29**, 123–140.
- Simmons, D.M., Arriza, J.L. and Swanson, L.W. (1989) *J. Histotechnol.*, **12**, 169–181.
- Sternberg, D.W., Scholtz, G., Fukui, Y. and Hanafusa, H. (1993) *EMBO J.*, **12**, 323–330.
- Strasser, A., Harris, A.W. and Cory, S. (1991) *Cell*, **67**, 889–899.
- Sugano, S., Stoeckle, M.Y. and Hanafusa, H. (1987) *Cell*, **49**, 321–328.
- Tapley, P., Horwitz, A., Buck, C., Duggan, K. and Rohrschneider, L. (1989) *Oncogene*, **4**, 325–333.
- Taylor, S.J. and Shalloway, D. (1993) *Curr. Opin. Genet. Dev.*, **3**, 26–34.
- Vaux, D.L. (1993) *Curr. Biol.*, **3**, 877–878.
- Welham, M.J., Wyke, J.A., Lang, A. and Wyke, A.W. (1990) *Oncogene*, **5**, 161–169.
- Williams, G.T. and Smith, C.A. (1993) *Cell*, **74**, 777–779.
- Wood, K.A., Dipasquale, B. and Youle, R. (1993) *Neuron*, **11**, 621–632.
- Yin, X.M., Oltval, Z.N. and Korsmeyer, S.J. (1994) *Nature*, **369**, 321–323.
- Yoon, H. and Boettiger, D. (1994) *Oncogene*, **9**, 801–807.
- Zheng, X.M., Wang, Y. and Pallen, C.J. (1992) *Nature*, **359**, 336–339.

Received on November 7, 1994; revised on December 29, 1994